Georgia Tech

THE GEORGE W. WOODRUFF SCHOOL OF
MECHANICAL ENGINEERING

Georgia Institute of Technology
Atlanta, Georgia 30332-0405

October 18, 1991

TO: **Dr. Marvin Blizard, Scientific Officer,**
Office of Naval Research.

FROM: **Jacek Jarzynski, Professor,** Jacek Jarzynski
School of Mechanical Engineering.

SUBJECT: **FINAL REPORT TO THE OFFICE OF NAVAL RESEARCH under contract N00014-87-K-0021.**

The project under contract N00014-87-K-0021 entitled "Laser-Doppler Techniques for Sensing of Compressional Waves" was supported by funds from the Office of Naval Research during the period from October, 1986 to January, 1991. Initially Dr. Allan Pierce was the principal investigator. I became the principal investigator after Dr. Pierce left Georgia Tech in September, 1988. Other persons working on the above project were Dr. Yves H. Berthelot as a co-investigator, and Joseph Vignola, a graduate student whose work on this project was in partial fulfilment of the requirements for the Ph.D. degree.

I delayed the final report on the above project until Vignola's graduation. His Ph.D. thesis is now submitted as the final project report, together with a summary of accomplishments and a list of publications. Part of the above thesis was recently published in the Journal of the Acoustical Society, and a copy of this paper is included.

ACCOMPLISHMENTS and PUBLICATIONS

ACCOMPLISHMENTS

The research topic of the N00014 project was the remote sensing of sound waves in water from measurements of the Doppler shift in laser light scattered from microparticles suspended in the water. The main objective of the research was to develop, and experimentally verify, a theoretical model for the Laser Doppler (LD) technique. This theoretical model can be used to both predict and optimize the performance of the LD system. The major accomplishments of the above project, described in Vignola's thesis, are as follows:

(1) Polarization preserving fibers were used to design a system where the optical head unit (for transmitting and receiving the laser light) was compact and removed from the main optical bench (which contains the laser and other optical components). This design allows great flexibility for positioning and scanning the laser beam in the water.

(2) Special polystyrene microparticles were used in the experiments. These microparticles were very uniform in shape (spherical) and size. Three different sizes were used - 0.1μm, 1μm and 10μm radius. Very pure water (reverse osmosis) was used so that it could be seeded with just one known type of microparticle. Therefore, the experimental data could be directly compared with theoretical models for the LD system. Most of the measurements were made in the forward light scattering direction, where the scattered light intensity is maximum. However, some measurements were also made in the backscatter direction since this configuration has more practical applications.

(3) By using controlled size microparticles it was possible to study quantitatively the broadening in the frequency spectrum of the scattered light due to Brownian motion of the microparticles. The experimental data was consistent with the theoretical model of Clark et. al. (Am. J. Phys., **37**, 853, (1969) and **38**, 575, (1970)). The broadening due to Brownian motion is a small effect and is not likely to be a limiting factor in practical applications of the LD technique.

(4) A more accurate model was developed for the interaction between the vibrating fluid and the suspended microparticle (J.Vignola, Ph.D. thesis, Chapter 4). This model shows that a microparticle of given size and density will follow the fluid motion due to the sound wave over a much wider frequency range than previously estimated.

(5) A rigorous theoretical model was developed for the scattering of light from two beams incident from different directions on a spherical microparticle. This model uses the Mie theory (which is exact) of light scattering from a dielecric

sphere. The above model applies directly to the two beam LD system used in the present study. For a microparticle of given size this model can be used to estimate the intensity of light scattered in any given direction from each of the two beams, and hence estimate the contrast of the fringes formed by the interference of the two scattered light signals. In summary, the above model can be used to accurately estimate the signal to noise ratio for any configuration of the two beam LD system. The computer program for this model is available on request.

(6) A new procedure for data acquisition was studied (J.Vignola, Ph.D. thesis, Chapter 5, Section 9). This procedure uses recently developed digital data acquisition equipment. Data is collected only when the scattered light intensity exceeds a preset threshold value. Thus, data is collected only when a microparticle is present in the center region of the two beam overlap volume. The collected signal is digitized, transferred to a computer, and a Fast Fourier Transform is performed to determine the frequency spectrum of the scattered signal. This procedure gave a better signal to noise ratio and a more consistent frequency spectrum than the output obtained when an analog spectrum analizer was used to process the data from the photomultiplier.

All measurements in the present study were made with low densities of microparticles in the water, so that at any given time the light was scattered from a single microparticle in the overlap volume. Hovever, the results and models developed in the present study can be extended to the case of multiple particle scattering by using the formalism developed by George and Lumley (J. Fluid Mech., **60**, 321, (1973)).

PUBLICATIONS

Refereed Journals

J. Vignola, Y. H. Berthelot and J. Jarzynski, "Laser Detection of Sound," J. Acoust. Soc. Am., **90**, 1275-1286, (1991).

Conference Proceedings

J. Jarzynski, D. Lee, J. Vignola, Y. H. Berthelot and A. D. Pierce, "Fiber Optic Doppler Systems for Remote Sensing of Fluid Flow," Ocean Optics IX, ed by M. A. Blizard, SPIE Proceedings Vol.**925**, pp. 250-254, (1988).

J. Vignola, Y. H. Berthelot and J. Jarzynski, "Nonintrusive absolute measurements of acoustic particle velocity in fluids," Proceedings of the 13th International Congress on Acoustics, ed. P. Pravica, Vol.**4**, pp. 45-48, (1989).

Conference Presentations

A. D. Pierce, "Possibility of improved laser-Doppler detection of sound by tracking moving phase fronts," J. Acoust. Soc. Am., Suppl. 1, Vol. 82, Fall 1987.

A. D. Pierce and Y. H. Berthelot, "Absolute calibration of acoustic sensors utilizing electromagnetic scattering from in situ particulate matter," J. Acoust. Soc. Am., Suppl. 1, Vol. 83, Spring 1988.

J. Vignola, Y. H. Berthelot and J. Jarzynski, "Absolute Measurement of Particle Velocity of Time-Harmonic Acoustic Waves," J. Acoust. Soc. Am., Suppl. 1, Vol. 84, Fall 1988.

Laser detection of sound

Joseph F. Vignola, Yves H. Berthelot, and Jacek Jarzynski
School of Mechanical Engineering, Georgia Institute of Technology, Atlanta, Georgia 30332

(Received 17 June 1990; accepted for publication 23 April 1991)

A differential laser Doppler velocimeter (LDV) has been assembled and tested to provide noninvasive absolute measurements of acoustic particle displacements of standing waves generated in a water-filled tube. The principle of the technique [see K. J. Taylor, J. Acoust. Soc. Am. **59**, 691–694 (1976)] is to measure the Doppler shift of laser light scattered from colloidal microparticles oscillating under the action of an acoustic field. The system tested is capable of detecting particle displacements of the order of a few nanometers with a bandwidth of several kilohertz. The performances and limitations of the system are discussed. In particular, the effect of Brownian motion is shown to produce only negligible broadening of the spectral density of the signal of interest. The sensitivity of the present LDV system is estimated to be very close to the shot noise limit of the photomultiplier tube used to detect the Doppler shift of the scattered light. Experimental results are obtained under controlled laboratory situations with calibrated microparticles of radii 10, 1, 0.1, and 0.01 μm in suspension in very pure (reverse osmosis) water.

PACS numbers: 43.85.Fm, 43.88.Ar, 43.30.Es, 43.20.Tb

INTRODUCTION

The pioneering work of Yeh and Cummins[1] in 1964 demonstrated that lasers can be used to measure steady fluid velocities by observing the Doppler shift in the laser light scattered from small particles moving with the fluid. Since then, laser Doppler velocimetry (LDV) has become a standard tool for the noninvasive measurement of the small-scale structure of turbulence in fluids.[2] The basic premise associated with LDV measurements is that the fluid under investigation contains some microparticles (either natural impurities or seeded particles) that move with the local fluid velocity and scatter any incident light. Motion of the scatterers produces a Doppler shift of the scattered light which can be detected with appropriate electronics and signal processing. In 1973, George and Lumley[3] made a comprehensive study of the spatial and temporal resolutions of laser Doppler velocimeters and gave criteria for meaningful interpretation of measurements in the context of turbulence in fluids. A few years later, K. J. Taylor[4,5] successfully extended the LDV technique used in fluid mechanics to the area of acoustics by measuring in-air particle velocities associated with steady-state time-harmonic waves in standing-wave and traveling-wave tubes. His experiments were conducted in air where particle velocities are relatively high compared to particle velocities in water. Taylor also mentions taking data in water, but presents no experimental data.[4] The main difficulty in extending the LDV technique to acoustics is that acoustic quantities oscillate several thousand times every second (at frequencies in the kilohertz range) at velocities that, in water, can be as low as a few micrometers per second, and with amplitudes of displacement that can be as small as a few nanometers. Hanish[6] has compiled a review of the potential for developing "an underwater laser Doppler hydrophone" in his treatise on acoustic radiation. He gives the theoretical background for homodyne and heterodyne interferometric LDV systems as well as practical design considerations for a remote-sensing laser hydrophone. He addresses the issue of signal to noise ratio and minimum detectability of the LDV hydrophone. He also shows that, under certain circumstances, Brownian motion (i.e., thermal agitation in the fluid) can be a serious limitation. However, very little experimental[6-9] data are shown in his review or in the literature available on the subject.

The present study differs from previous publications, and includes original contributions, as follows: (1) a comparison of different ways of data acquisition including the use of state of the art digital techniques; (2) a discussion and comparison of the observed minimum detectable signal level with the theoretically predicted (shot noise limited) minimum detectable level; and (3) an experimental and theoretical study (using calibrated microparticles of different sizes) of the effect of Brownian motion of the microparticle on measurements of the acoustic signal.

The objective of this paper is first to present experimental data obtained with state of the art technology in order to study the fundamental limitations of LDV systems for the detection of underwater sound. Section I is devoted to the basic theoretical framework necessary for understanding the experiment and for meaningful interpretation of the data. In particular, special attention is given to the derivation of the equations describing the effect of Brownian motion on the measured data. Section II is a detailed discussion of the experiment conducted in our laboratory. It includes: a description of the prototype LDV system; considerations on the optical fibers being used in the experiment; the design of a mechanical mounting of miniature lenses used to collimate the laser beams leaving the fibers; a description of the standing wave tube and driving sound source; comments regarding the preparation of carefully controlled water samples seeded with calibrated microparticles; and some details on the signal processing techniques used to analyze the data. Experimental results are presented in Section III. It is shown

 0001-4966/91/091275-12$00.80

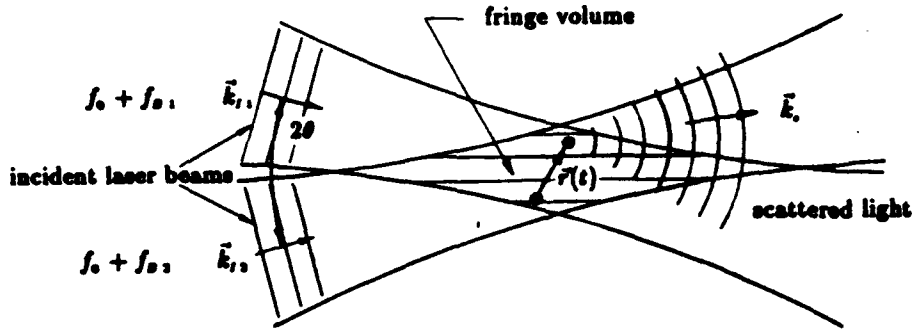

FIG. 1. Two laser beams of optical wave vectors $\mathbf{k}_{I1}$ and $\mathbf{k}_{I2}$ are incident on a moving scatterer whose position is $\mathbf{r}(t)$. The light scattered in a given direction θ, is represented by the wave vector $\mathbf{k}_s$.

that the laser detection of underwater sound is quite feasible, although it is not as sensitive as other more conventional techniques would be, and that Brownian motion is not a major concern for practical applications.

I. THEORY

Consider a fluid with either natural impurities or calibrated particles present in suspension with a time-harmonic acoustic wave of amplitude A_m. The sound wave produces an oscillation of the suspended particles with an amplitude of A_p. Brandt *et al.*[10] have shown that the ratio of the amplitude of the particle displacement relative to the acoustic particle displacement is

$$A_p/A_m = \{1 + [(4\pi\rho_\omega/9\mu)a^2\gamma_\rho f_a]^2\}^{1/2}, \quad (1)$$

where ρ_ω and μ are the density and viscosity of water, a and γ_ρ are the radius and specific gravity of the particle, and f_a is the acoustic frequency in hertz. As a result, it is expected that neutrally buoyant particles with radii less than 10 μm will oscillate with an amplitude which is 95% of the displacement of the surrounding water for acoustic frequencies less than 2500 Hz.

In general, the displacement of the microparticles in the fluid includes, in addition to the acoustic displacement, any macroscopic fluid motion and the motion of the particle due to the random impacts with the molecules in the surrounding fluid (Brownian motion). As a consequence of the motion of the particle, any laser light incident on the particle produces scattered light which is Doppler shifted. The theory of the laser detection of sound is based on deducing the acoustic particle displacement (or velocity) from measurements of the Doppler shift of laser light scattered by microparticles that acted as scatterers, in suspension in a fluid in which acoustic wave motion is present.

A. Arbitrary particle motion r(t)

Consider a single scatterer whose position is described by the time-varying vector $\mathbf{r}(t)$. At time $t = 0$, a small particle is assumed to be at an arbitrary origin O. Let the particle be illuminated simultaneously by two laser beams of slightly different optical frequencies $f_0 + f_{B1}$ and $f_0 + f_{B2}$, from different directions, as is shown in Fig. 1. Here, f_0 is the optical frequency of the laser light, typically of the order of 10^{14} Hz, and f_{B1} and f_{B2} are the induced frequency shifts, typically several MHz, imposed by the acousto-optic Bragg cells present in heterodyne LDV detection systems.[11,12] The purpose of the Bragg shifts in the laser frequency is to produce beating at the frequency $f_{B1} - f_{B2}$ at a point in the region where the two laser beams intersect. This region is referred to as the fringe volume. Let $\mathbf{k}_{I1}$ and $\mathbf{k}_{I2}$ be the wavevectors of the two incident laser beams and $\mathbf{k}_{S1}$ and $\mathbf{k}_{S2}$ the scattered wave vectors in the direction of a receiver. For a receiver located many optical wavelengths away from the fringe volume, $\mathbf{k}_{S1}$ and $\mathbf{k}_{S2}$ are identical; therefore, the distinction is unnecessary and we can let $\mathbf{k}_S = \mathbf{k}_{S1} = \mathbf{k}_{S2}$. The motion of the particle introduces an optical phase shift $\Delta\phi_i$ for the light scattered from each of the beams ($i = 1,2$). This phase shift, observed at the receiver, is given by

$$\Delta\phi_i = (\mathbf{k}_{Ii} - \mathbf{k}_S)\cdot\mathbf{r}(t). \quad (2)$$

The total electric field at the receiver E is the sum of the electric fields scattered from each beam:

$$E = E_1 \cos[(\omega_0 + \omega_{B1})t + \Delta\phi_1] + E_2 \cos[(\omega_0 + \omega_{B2})t + \Delta\phi_2 + \Delta\phi_r(t)], \quad (3)$$

where E_1 and E_2 are the magnitudes of the electric fields of the light scattered by the particle from each beam. The term $\Delta\phi_r(t)$ is the difference in phase of the two beams due to unequal path lengths in the two arms of the interferometer. Because of thermal effects present in any realistic experimental apparatus that incorporates optical fiber, this term is usually a slowly varying function of time. To examine the effect of the particle motion on the scattered electric field, Eq. (3) is rewritten in magnitude-phase form as follows:

$$\begin{aligned} E &= [E_1^2 + E_2^2 + 2E_1E_2\cos(\omega_d t + \Delta\phi_2 - \Delta\phi_1 + \Delta\phi_r)]^{1/2} \\ &\quad \times \cos[(\omega_0 + \omega_d)t + \phi_0] \\ &= K(t)\cos[(\omega_0 + \omega_d)t + \phi_0], \end{aligned} \quad (4)$$

where ϕ_0 is the optical phase of received light given by

$$\phi_0 = \tan^{-1}\left(\frac{E_1\cos\Delta\phi_1 + E_2\cos(\omega_d t + \Delta\phi_2 + \Delta\phi_r)}{E_1\sin\Delta\phi_1 + E_2\sin(\omega_d t + \Delta\phi_2 + \Delta\phi_r)}\right). \quad (5)$$

In Eqs. (4) and (5), $\omega_d = 2\pi(f_{B2} - f_{B1})$ is the difference of angular frequency of the two beams and is the angular

frequency at which beating occurs in the fringe volume. The receiver is a photodetector such as a photodiode or photomultiplier which produces an electrical current proportional to the square of the magnitude of the incident electric field. These devices do not respond at the optical frequencies, and, as a consequence, the output of the photodetector is derived only from the first part of Eq. (4), i.e., only from the coefficient $K(t)$. Ignoring the dc component $(E_1^2 + E_2^2)$, one can write an dimensionless expression for the current, $I_N(t)$:

$$I_N(t) = \cos(\omega_d t + \Delta\phi + \Delta\phi_r). \tag{6}$$

In this equation the term $\Delta\phi_2 - \Delta\phi_1$, which is rewritten as $\Delta\phi$, is the phase fluctuation due to all motion of the scattering particle (including acoustic displacement, Brownian motion, flow-induced drift, and other motions). From Eq. (2) $\Delta\phi$ can be expressed as $\Delta\phi = \mathbf{k}\cdot\mathbf{r}(t)$, where $\mathbf{k} = \mathbf{k}_{I1} - \mathbf{k}_{I2}$. The general expression for the normalized intensity received at the photomultiplier can be written as

$$I_N(t) = \cos[\omega_d t + \mathbf{k}\cdot\mathbf{r}(t) + \Delta\phi_r(t)]. \tag{7}$$

Let $k = |\mathbf{k}_{I1} - \mathbf{k}_{I2}|$ be the magnitude of the difference of the two incident wave vectors and $|\mathbf{r}(t)|$ be the magnitude of the particle displacement. The normalized intensity at the photodetector is then rewritten as

$$I_N(t) = \cos[\omega_d t + k\,|\mathbf{r}(t)|\sin\theta_r + \Delta\phi_r(t)]. \tag{8}$$

In Eq. (8), θ_r is the orientation of the particle displacement vector and is the complement of the angle between $\mathbf{r}(t)$ and $\mathbf{k}$. By evaluating k in terms of physical parameters, it is found that k is $4\pi n_0 \sin\theta/\lambda$. In this expression, n_0 is the optical index of refraction of the suspending fluid, θ is the half-angle between the two incident light rays, and λ is the *in-vacuo* wavelength of the laser that produces the incident light beams. From Eq. (8) it can be seen that change of phase of the light which reaches the receiver is affected only by the component of the particle displacement in the direction perpendicular to the bisector of the two incident beams. The change in wavelength imposed by the two Bragg shifts f_{Bi} in each beam is neglected because in any realistic configuration $f_{Bi}/f_0 \ll 1$. Equation (8) is the basis for the detection of any particle motion $\mathbf{r}(t)$ with an LDV system. This equation shows that the photomultiplier output current is a carrier signal at the difference Bragg frequency ω_d modulated by a signal proportional to the instantaneous motion of the particle in terms of the optical wavelength. An important result is that the intensity at the photomultiplier does not depend on its angular position, or that $I_N(t)$ is independent of the direction of $\mathbf{k}_S$. Hence, one should collect as much scattered light as possible, by using a large aperture collecting lens. Another important conclusion which can be drawn from Eq. (8) is that motion parallel to the bisector of the two beams ($\theta_r = 0$) cannot be detected. Conversely, the modulation signal from the photomultiplier is increased when the angle between the two incident laser beams is increased.

B. Time-harmonic particle displacement

The simplest sound field to study is that produced by a standing wave. Let a sound wave of acoustic particle displacement $A\sin\omega_a t$ be incident on the scatterer along the y axis. Here, A and ω_a are, respectively, the amplitude and the angular frequency of the acoustic wave that one is trying to detect. In this simple case, the motion of the scatterer in the fringe volume is along the y axis ($\theta_r = 90°$) and the particle motion is given by $r(t) = A\sin\omega_a t + r_{Br}(t)$, where $r_{Br}(t)$ is the y component of the particle displacement due to Brownian motion. By substituting this expression that describes the particle motion into Eq. (8), photomultiplier signal may then be expressed as

$$I_N(t) = \cos[\omega_d t + C\sin\omega_a t + S(t)], \tag{9}$$

where $C = 4\pi n_0 \sin\theta(A/\lambda)$, the amplitude of the phase modulation, or phase amplitude of the light intensity signal and is a measure of the acoustic displacement in terms of an optical wavelength. The phase term of Eq. (9) also contains the random fluctuation $S(t) = \Delta\phi_{Br} + \phi_r$ due to Brownian motion of the particle and thermal expansion of the optical fibers. The phase fluctuation due to the Brownian motion is given by $\Delta\phi_{Br} = kr_{Br}(t)\sin\theta_r$, which is directly proportional to the projection on the y axis of the instantaneous vector displacement, $\mathbf{r}_{Br}(t)$, due to Brownian motion. The photomultiplier output intensity is a harmonic carrier signal at the difference frequency of the two Bragg cells modulated by a time harmonic signal of angular frequency ω_a with a random phase fluctuation. In order to estimate the frequency content of such a signal, Eq. (9) is customarily expressed as a series of Bessel functions of the first kind and order n:[13]

$$\begin{aligned} I_N(t) = {} & J_0(C)\cos(\omega_d t + \Delta\phi_{Br} + \Delta\phi_r) \\ & + \sum_{n=1}^{\infty} J_n(C)\cos[(\omega_d + n\omega_a)t + \Delta\phi_{Br} + \Delta\phi_r] \\ & + \sum_{n=1}^{\infty} (-1)^n J_n(C)\cos[(\omega_d - n\omega_a)t \\ & + \Delta\phi_{Br} + \Delta\phi_r]. \end{aligned} \tag{10}$$

It follows that, in the frequency domain, $I_N(t)$ has a center peak, referred to as the Bragg peak, at $\omega_d = \omega_{B2} - \omega_{B1}$, given by the first term in the above equation. The remaining terms in this equation represent higher-order peaks, referred to as sidebands. These sidebands are a direct consequence of the acoustic disturbance and occur at angular frequencies of $\omega_d \pm n\omega_a$, where ω_a is the angular frequency of the time-harmonic sound wave.

The argument C of the Bessel functions in Eq. (10) is the amplitude of the phase modulation from Eq. (9). It can be determined from the ratio J_1/J_0 of Bessel functions. Because C is a measure of the acoustic particle displacement relative to the wavelength of the laser light, it establishes the acoustic particle displacement in terms of known quantities. When the acoustic particle displacement A is much less than the optical wavelength λ, the phase modulation amplitude C is much less than unity. The Bessel function can be approximated by using the small argument limits $J_0(C) \simeq 1$ and $J_1(C) \simeq C/2$. The ratio of the amplitude of the first-order side peak to the Bragg center peak is

$$\text{ratio} = \frac{J_1(C)}{J_0(C)} \simeq \frac{C}{2} = \frac{2\pi n_0 A}{\lambda}\sin\theta. \tag{11}$$

The above discussion indicates that a spectral analysis of the light intensity received at the photomultiplier allows one to

determine both the acoustic frequency ω_a and the amplitude A of the particle displacement in a single absolute measurement. Since the particle displacement is found from a ratio quantity that relates the acoustic displacements to the wavelength of light, no calibration is required to get its absolute measurement.

It appears from Eq. (10) that the slowly time-varying random phase fluctuation $\Delta\phi_r$ affects in a similar fashion each peak of the photomultiplier intensity spectrum. In fact, it can be shown (for instance, by computer simulation) that the effect of random processes such as those represented by the Brownian motion term $\Delta\phi_{Br}$ and the thermal expansion term $\Delta\phi_r$ is to broaden the width of the spectral peaks of the photomultiplier intensity signal. It has been suggested[3,6] that spectral broadening resulting from Brownian motion could be a fundamental limitation of the LDV detection system. In the worst case, spectral broadening due to Brownian motion might be such that the half-width of the Bragg peak is greater than the acoustic frequency that one wants to detect. In this case, Hanish warned that the acoustic peak would be obliterated by the Bragg peak. This issue is discussed in detail in the present article. In particular, the next section is devoted to establishing an analytical expression for predicting the spectral broadening due to Brownian motion.

C. Spectral broadening due to Brownian motion

In 1969, Clark *et al.*[14,15] reported on a study of Brownian motion with an LDV system. The following analysis is based on Clark's formulation for the spectral broadening due to Brownian motion. In this section we consider the effect of the random phase fluctuations due to Brownian motion on the beat signal from the photomultiplier with no acoustic wave present in the system. The reason is that Eq. (10) indicates that Brownian motion affects in the same way as the Bragg peak and the higher-order peaks. An understanding of the broadening of the Bragg peak is therefore all that is needed to quantify the effect of Brownian motion on the spectral content of the photomultiplier intensity.

The first step in this development is to evaluate the correlation function $R_I(\tau)$ for the current output from the photomultiplier $I_N(t)$. If one neglects the slowly time-varying random process $\Delta\phi_r$ attributable to the thermal expansion of the optical fiber to concentrate only on the effects of Brownian motion, it can be seen from Eq. (6) that

$$I_N(t) = \cos[\omega_d t + \Delta\phi_{Br}(t)]. \tag{12}$$

The correlation function is defined by

$$R_I(\tau) = \langle I_N(t) I_N(t+\tau)\rangle, \tag{13}$$

where $\langle\ \rangle$ denotes a time average over a long period of time T. Combining Eqs. (12) and (13) and using a simple trigonometric identity yields

$$R_I(\tau) = \tfrac{1}{2}\langle\cos[\omega_d\tau - \Delta\phi_{Br}(t) + \Delta\phi_{Br}(t+\tau)]\rangle + \tfrac{1}{2}\langle\cos[2\omega_d t + \omega_d\tau + \Delta\phi_{Br}(t) + \Delta\phi_{Br}(t+\tau)]\rangle. \tag{14}$$

The second term in Eq. (14) averages to zero as the limits of the integration become large because it is a rapidly varying function of time t. Since

$$\Delta\phi_{Br}(t+\tau) - \Delta\phi_{Br}(t) = \mathbf{k}\cdot[\mathbf{r}(t+\tau) - \mathbf{r}(t)], \tag{15}$$

a more compact notation may be employed for Eq. (13) using

$$\Delta\phi_{Br}(t+\tau) - \Delta\phi_{Br}(t) = \mathbf{k}\cdot\Delta r, \tag{16}$$

to express the difference of the phase terms. The correlation function reduces to

$$R_I(\tau) = \lim_{T\to\infty}\frac{1}{2T}\int_{-T/2}^{T/2}\cos(\omega_d\tau + \mathbf{k}\cdot\Delta r)\,dt. \tag{17}$$

Rather than trying to evaluate this integral, which contains a random variable, Δr, over all time t, one can introduce the probability density of finding the particle at a distance $|\Delta r|$ from the origin after a given time τ. This probability density is denoted by $P(|\Delta r|;\tau)$. The purpose of this manipulation is to shift the variable of integration from τ to Δr. The time integration of the correlation function is thus replaced by a volume integration over all space. Since the probability density is defined by

$$\int_{-\infty}^{\infty}\int_{-\infty}^{\infty}\int_{-\infty}^{\infty} P(|\Delta r|;\tau)\,d^3(\Delta r) = 1, \tag{18}$$

the correlation function is rewritten as

$$R_I(\tau) = \frac{1}{2}\int_{-\infty}^{\infty}\int_{-\infty}^{\infty}\int_{-\infty}^{\infty} P(|\Delta r|;\tau) \times\cos(\omega_d\tau + \mathbf{k}\cdot\Delta r)\,d^3(\Delta r), \tag{19}$$

where the probability density is the three-dimensional generalization[16] of the one-dimensional version initially derived by Einstein:[17,18]

$$P(|\Delta r|;\tau) = \frac{1}{(4\pi D\tau)^{3/2}}\exp\left(\frac{-(|\Delta r|)^2}{4D\tau}\right). \tag{20}$$

In the above equation, D is the diffusion coefficient or diffusivity of the microparticle. For a spherical particle D is given by Eq. (21) below, known as the Einstein–Stokes relation[19,20]

$$D = k_B T/6\pi\mu a, \tag{21}$$

where k_B is Boltzmann's constant, T is the absolute temperature, a is the radius of the microparticle, and μ is the viscosity of the solvent in which the microparticle is in suspension. By evaluating the integral of Eq. (19) in spherical coordinates, one can derive an expression for $R_I(\tau)$ that does not contain any random variables:

$$R_I(\tau) = \cos(\omega_d\tau)\exp(-k^2 D|\tau|), \tag{22}$$

where $k = 2|\mathbf{k}|\sin\theta$, θ being the half-angle between the incident beams. [Note that this differs from Clark's[14,15] definition of k, which is $k = 2|\mathbf{k}|\sin(\theta/2)$. This is due to the fact that we are using a differential[11] optical configuration, whereas he used a direct configuration.] The effect of Brownian motion appears in the Gaussian exponential. The Wiener–Khintchine theorem[21] states that the Fourier transform (denoted by $\mathcal{F}$) of the correlation function $R_I(\tau)$ is defined as the power spectral density $S_I(\omega)$ of the current signal from the photomultiplier. It is found to be

$$\mathcal{F}\{R_I(\tau)\} = S_I(\omega) = 2k^2 D/[(\omega-\omega_d)^2 + (k^2 D)^2]. \tag{23}$$

Equation (23) describes what is referred to as a Lorentzian spectrum.[22] It can be seen that the width of the Bragg peak in the LDV system (and consequently of any other higher-order spectral peaks) is broadened according to the Lorentzian distribution of Eq. (23). It follows that the full width at half-height of any given peak of the spectral density of the signal is[14,15]

$$\Delta f_{1/2} = \frac{k^2 D}{\pi} = \frac{8}{3}\left(\frac{n}{\lambda}\right)^2 \frac{k_B T}{\mu a} \sin^2 \theta, \tag{24}$$

where n is the refraction index in the fluid. This measure of spectral broadening due to Brownian motion indicates that, even for particles as small as 0.1 μm in radius in suspension in water at room temperature, the spectral broadening $\Delta f_{1/2}$ is only a few hertz. Consequently, Brownian motion may not be a serious limitation in the detection of underwater sound as had been suggested earlier.[6] Carefully controlled experiments have been conducted to resolve the issue of Brownian motion. The results are discussed in Sec. III.

II. EXPERIMENT

A. Prototype LDV system

The LDV apparatus used in this study is a dual beam system[11,12] operating in the differential heterodyne mode. The laser beam is split into two beams, referred to as the arms of the interferometer. Each beam is subsequently frequency shifted by acousto-optic Bragg modulation (heterodyne detection). The beams cross in the region (referred to as the probing or fringe volume) where one wants to detect sound. Light scattered from small particles in suspension in the probing volume is collected by a large aperture lens and focused toward an optical detector. A measure of the Doppler shift of the scattered light is an indirect measure of the velocity of the small particle and, in most practical cases, a good measure of the acoustic particle velocity of the sound wave.

Figure 2 shows the system set up in a forward scattering configuration, that is to say, when the optical detector is located straight ahead of the incident laser beams, on the axis of symmetry. A one watt cw argon laser, set to operate in a single mode, (optical wavelength in air 514.5 nm) produces a ray of light with power ranging from about 10–500 mW. The linearly polarized light ray is split into two beams by a nonpolarized beam-splitting cube. The two light beams of nearly equal intensity are then passed through acousto-optic Bragg cells. The Bragg cells shift the optical frequency of the light by diffracting it from a traveling acoustic wave in a crystal.[23] In our experiment, one of the beams is shifted by 40.000 MHz and the other by 40.050 MHz. The frequency synthesizers driving the Bragg cells at these frequencies are stable within 40 Hz. Beating at the difference frequency, $\Delta f_B = 50.0$ kHz, occurs when these beams cross. This difference frequency is selected to satisfy sampling requirements that will be discussed later. The two beams are directed through apertures that block all but the first diffraction order from the Bragg cells so that only the beams shifted by 40 and 40.05 MHz are used in the interferometer. The frequency-shifted beams are then coupled into two single mode polarization preserving optical fibers (core diameter 4 μm, numerical aperture of 0.3) through a pair of microscope objectives (magnification 20×) that are mounted on positioners designed to couple efficiently the light beams into the fibers. The fibers (about 2 m long) guide the light to the detection bench, which is isolated from the optical bench. The light that emerges from each of the fibers is collimated by a miniature cylindrical lens (1.9-mm diameter, 16.5 mm long) with a graded index of refraction referred to as a GRIN lens. The length of the GRIN lens is such that a light spot illuminating the center of one side of the cylindrical

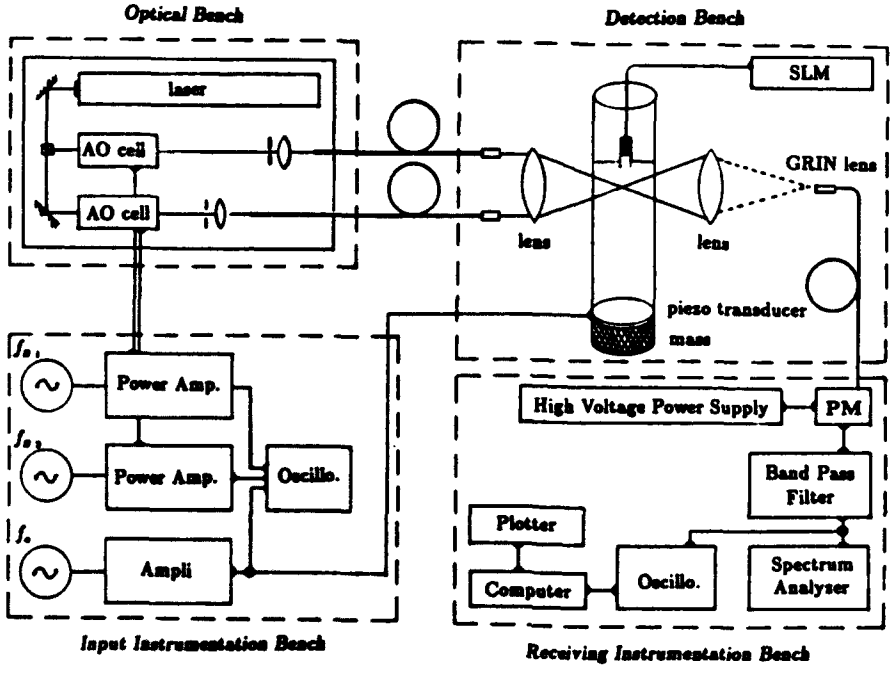

FIG. 2. Block diagram of the experimental apparatus used in the laser detection of sound in a standing wave tube filled with water.

GRIN lens leaves the other side of the lens perfectly collimated. Such a lens is called a quarter-pitch lens. The reverse is also true and GRIN lenses can be used to efficiently couple a collimated light beam into a single mode or a multimode optical fiber. A detailed discussion of the mechanical coupling between the miniature GRIN lens and the optical fiber is given in Sec. II C. The light from both beams is linearly polarized in the same plane in order to achieve a high contrast in the probing volume where the two beams intersect to create the fringe pattern. Good contrast is required to ensure good signal-to-noise ratio at the detection stage. A detailed procedure on the method used to align properly the polarization axes of the two fibers is given below in Sec. II B. A large aperture (127-mm diameter) converging lens focuses the two beams to a common focal point (about 30 cm away) in the center of a clean water-filled stainless steel cylindrical standing wave tube (3.8-cm i.d., 6.3-cm o.d.). A detailed description of the standing wave tube is given in Sec. II D. The water inside the tube is carefully controlled so that impurities remaining in the fluid are sufficiently small that they scatter a negligible amount of light. The purified water is then seeded with polystyrene microparticles of known radius (either 10, 1, or 0.1 μm, corresponding to values of ka of 183, 18.3, and 1.83, respectively), which act as calibrated scatterers of light. The density of the microparticles is about 1050 kg/m^3 (specific gravity 1.05); the particles are therefore in suspension in the water. The water sample preparation is discussed in Sec. II F below. A piezoelectric transducer generates a single frequency sound wave into the water. The sound wave induces motion of the scatterers and consequently a Doppler shift in the light scattered from the buoyant microparticles. The light scattered in the forward direction is collected and focused by another large aperture lens (127-mm diameter). Another miniature GRIN lens is placed at the point where the light is focused to couple the scattered light to a multimode optical fiber (100-μm diameter). The multimode optical fiber guides the collected light to a ten stage Thorn 9903 KB photomultiplier tube (22% quantum efficiency) that produces a signal proportional to the incident light intensity. This signal, which is related to the Doppler shift of the light, is then bandpass filtered and amplified so that the motion of the particles can be determined. Details concerning the signal processing can be found in Sec. II G below.

B. Alignment of the polarization preserving optical fibers

The design of the prototype system takes advantage of the flexibility that optical fibers provide: ease of alignment, and decoupling of the optical bench from the area that is being investigated. Another advantage is that polarization-preserving fibers are now available and can be used to maximize the efficiency of the LDV system by sharpening the contrast between the fringes in the interference region where the laser beams cross. Ordinary optical fibers do not maintain polarization during transmission over long distances.[24] Polarization-preserving fibers, however, are made of a birefringent core and, consequently, when linearly polarized light enters the fiber with its electric field vector oriented along one of the principal axes of the fiber, it emerges linearly polarized.[25]

To take advantage of this type of optical fiber, a systematic approach was developed to align the optical axes of the polarization preserving fiber so that the light that emerges from the fiber is linearly polarized (the electric field vector propagates in a fixed plane). The light emitted by the laser is linearly polarized vertically. A microscope objective mounted on a specially designed positioner was used to focus the light onto the core of the single mode polarization preserving fiber. The inlet side of the fiber is mounted on a rotator on the same positioner, thus allowing the fiber to be placed so that the laser light is focused directly on the core of the fiber. If the optical axis of the fiber is not aligned with the axis of polarization of the incident light, the light that emerges is elliptically polarized because the polarization-preserving fiber is birefringent. It is therefore necessary to align one of the principal axes of polarization of the fiber with the plane of polarization of the incoming laser light. This is achieved by placing a polarizer at the output of the fiber and rotating the polarizer until the output light intensity becomes a minimum. The fiber is then slightly heated simply by holding it. This heating has an effect (the birefringence effect) on the velocities of propagation of both components of the light in the fiber[26] and induces a phase difference between the two components of light, which results in a change in intensity, due to interference, of the light after it passes through the polarizer. The proper orientation of the input side of the fiber is obtained iteratively by rotating the input side of the fiber until heating has no effect on the fiber's output intensity after it passes through the polarizer. At this point, when all of the light is propagating along one axis of the fiber, there will be no component of light along the other axis, therefore heating would not influence the output intensity. With the inlet side aligned, it is a simple task to use a polarizer to orient the outlet side of the fiber. The two fibers are cut to about the same length so that the difference in optical path length of the two arms of the system is well within the coherence length of the laser. The fibers are also kept close together so that thermal expansion effects are the same in both fibers. These measures insure sharp contrasts in the interference region and minimize fading and low-frequency noise associated with thermal fluctuations.

C. Mechanical mounting of the GRIN lenses

When using optical fiber, it is crucial that the light beam that emerges be well collimated. A miniature gradient index (GRIN) lens[27] that focuses light via its nonuniform index of refraction is chosen to insure proper collimation. Initially,

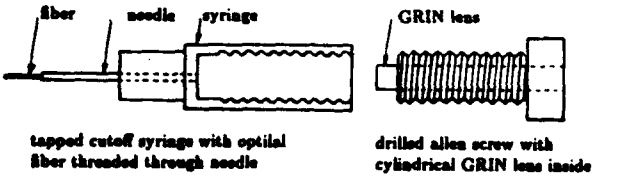

FIG. 3. Mechanical mounting and coupling of the miniature GRIN lens with a single-mode optical fiber.

the optical fiber was bonded to the GRIN lens with optical adhesive. However, the heat induced by the laser light at power levels of 100 mW and higher would melt the connection between the fiber and the GRIN lens, so a design for a mechanical mounting was pursued. The final design is shown in Fig. 3. A 27-gauge hypodermic needle and a half-inch-long Allen screw are used. The screw has a hole drilled through the center of the long axis so that the GRIN lens can fit inside with about 0.001 in. of clearance. Paraffin wax is used to hold the lens within the screw without stressing the lens. The screw is then threaded into a tapped syringe cut off about a half-inch into the cylinder portion. An optical fiber is inserted through the sharp side of the syringe and held in place with wax. Turning the screw causes the lens to move toward or away from the fiber and makes it possible to focus the light into a collimated beam.

D. Standing wave tube

The sound wave that is being detected with the LDV system is generated by a piezoelectric transducer located at the bottom of a vertically standing tube filled with water seeded with calibrated microparticles. Initially a 50.8×50.8 mm (2×2 in.) square tube made from two half-inch aluminum plates and two quarter-inch Plexiglas plates was built and used as a standing wave tube. Preliminary measurements of the sound field inside the tube were taken with a custom-made spherical ($\simeq 0.6$ cm in diameter) piezoelectric transducer. These measurements revealed a reduction in sound speed and the formation of spurious acoustic modes due to the high compliance and lack of mass in the walls of the tube, necessitating a redesign.

In an attempt to circumvent this problem, an alternative standing wave tube was constructed. The design was inspired by work done for impedance measurements in water made by Walter Kuhl in the 1940s.[28] Kuhl emphasizes the need for massive materials when building an impedance tube that will be filled with a liquid. Based on these considerations, the final design of our standing wave tube is a 29.2 cm (11.5 in.) tall stainless steel pipe with an inner diameter of 3.81 cm (1.5 in.) and a 1.27-cm (0.5 in.)-thick wall. It is shown in Fig. 4. The laser beams enter and exit through small Plexiglas windows in opposite sides of the pipe. These windows are circular with diameters of 1.90 cm (3/4 in.) and 1.90 cm (3/4 in.) thick. In this design, no glues or sealants are used in order to prevent impurities from leaching out into the water, thus maintaining the high degree of purity necessary in these experiments. At the base of the wave tube a thin and flexible stainless steel plate is secured to the bottom using a 0.95-cm (3/8 in.)-thick slice of the pipe material to sandwich the thin plate and seal the end. As indicated in Fig. 4, two stacked circular piezoelectric transducers are glued to the outer surface of the bottom so that they are not in the wave tube. A lead weight acting as an inertial mass was glued beneath the two transducers so that the excitation from the transducers would be directed upward into the standing wave tube. Suspending the transducers and weight from the flexible bottom plate of the wave tube minimizes the vibration transmission to the optical rail on which the standing wave tube and the two large converging lenses are

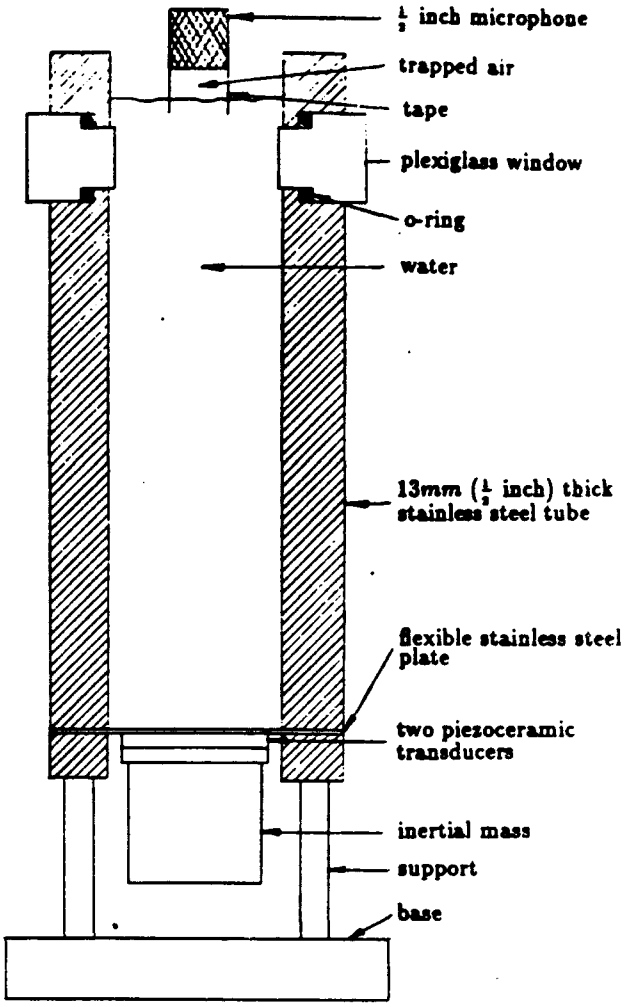

FIG. 4. Standing wave tube used in the experiment of laser detection of sound. A piezoelectric transducer produces a standing wave in the water filled pipe. A microphone is used at the free surface to estimate independently the particle velocity near the free surface for comparison with the LDV measurement.

placed. The wave tube is filled with water to a level just above the Plexiglas windows, approximately 15 cm (6 in.) from the bottom of the tube. The top of the water column is pressure release so that it can be driven at the quarter-wave resonance. This resonance is at a frequency well below the cutoff frequency (22.6 kHz). By driving at a frequency below the cutoff frequency, plane wave propagation is guaranteed.[29] The resonance condition is found experimentally by using the microphone system that is described in the next section.

E. Independent measurement of acoustic particle velocity

To verify the data obtained by the LDV system, an independent system for measuring the acoustic particle velocity was developed. The measurement is based on the assumption that the displacement velocity at the water surface is

essentially identical to the acoustic particle velocity in the fringe volume which is only 6 mm (1/4 in.) below the water surface, i.e., a fraction of an acoustic wavelength in water. The method is illustrated in Fig 4. A 1/2 in. Larson–Davies microphone is placed a small distance h above the surface of the water. The microphone has a plastic tape skirt placed on it to form the wall of a cylinder that traps a small volume V of air between the microphone and the water surface. Assuming adiabatic conditions and a rigid boundary at the tape skirt, one can regard the water as a piston compressing the trapped air. Since the wavelength of the sound in air is always kept large relative to the height of the air cylinder h, the peak acoustic pressure in the air volume p_a, which is measured by the microphone, can then be related to the surface displacement A_s, through a thermodynamic analysis which leads to the following:

$$A_s = (V/\gamma p_0 S_m)p_a = (h/\gamma p_0)p_a, \tag{25}$$

where $\gamma = 1.4$ is the ratio of the specific heats of the air, $p_0 = 101.5$ kPa is the ambient pressure, S_m is the surface area of the face of the microphone, and $h \simeq 6$ mm is the height of the trapped air cylinder under adiabatic compression. The acoustic pressure p_a in the trapped volume of air is measured directly by the microphone via the Larson–Davies 800B sound level meter. It is clear that this method for estimating the particle velocity in the fringe volume is not as accurate as the Doppler interferometric measurement, mainly because of the uncertainty of the precise volume of air trapped between the microphone, the surrounding tape, and the water surface. This measurement technique is intended to provide, first, a method for finding the resonance in the wave tube and, second, an order of magnitude value of the particle velocity at the pressure release end of the tube which can be compared with more accurate measurements obtained with the LDV system. The results of the comparison are shown in Sec. III.

F. Water sample preparation

When LDV data were collected from tests conducted in the standing wave tube, the tube was meticulously cleaned with soap and tap water and then carefully rinsed and filled with reverse osmosis water. For the study of the effect of Brownian motion, it was imperative that the light be scattered by particles of known size and shape. To achieve this, calibrated spherical polystyrene particles[30] were used to seed the water samples. These particles have a density of about 1050 kg/m^3. Their diameters are calibrated to be 220 $nm \pm 6\,nm$, $2.062\,\mu m \pm 0.025\,\mu m$, or $19.58\,\mu m \pm 0.10\,\mu m$. The neutrally buoyant particles are seeded in a controlled concentration, such that there is on average one particle in the fringe volume at a given time. In past experimental work, it was found that both distilled water or deionized water had sufficient levels of naturally occurring microparticles to produces a measurable signal from the photomultiplier prior to the seeding. To obtain a condition where no signal was present, a test tube was put in place of the standing wave tube. The test tube was carefully washed in a clean room and filled with reverse osmosis water that had been rapidly passed through a syringe filter and sealed. These test tubes were tested to see if they scattered light. When a test tube was then found to be clean, a controlled amount of scattering particles was added to the sample. It was not necessary to impose an acoustic disturbance on the sample because, as can be seen from Eq. (10), the random phase fluctuations caused by the Brownian motion broaden the Bragg peak in the same way they broaden the acoustic side peaks.

G. Signal processing

The light scattered from the microparticles in suspension in the water-filled wave tube is collected by a large aperture lens and focused via a quarter-pitch miniature GRIN lens into a mutimode optical fiber. The signal is carried through the optical fiber to a photomultiplier (Thorn EMI) driven with a high-voltage power supply. The signal is then amplified (52.2 dB) and bandpass filtered between 45 and 55 kHz. Initially data were analyzed directly with an HP 3285A spectrum analyzer. This approach, however, proved to be inadequate since the time required to collect data over even the narrow part of the spectrum of interest in this application is between 10 and 300 s, which is much longer than the typical duration of single scattering event. It was indeed apparent that the signal observed on the spectral analyzer was due to the scattering of many microparticles crossing the fringe volume and not due to a single scattering event as it should be for a meaningful interpretation of the results. In particular, the data displayed on the spectrum analyzer would show that the acoustic side peaks would not remain displayed continuously. The occurrence of a scattering event could easily be monitored simultaneously on an oscilloscope. A typical scattering event has a duration of a few hundred milliseconds and appears as a strong burst on the oscilloscope. In order to avoid the inherent averaging present in the display of the data on the spectrum analyzer, it was decided to collect data and store it in digital form only when a strong burst indicating a single scattering event would occur. A waveform recorder (HP 5180a) was used to collect data because of its ability to record signals using as many as 16 384 data points allowing for fine resolution in the frequency domain. By triggering the data acquisition only when a signal was above a certain threshold, one could surmise that the scattering conditions in the fringe volume were optimal. The waveform recorder sampling rate was 200 kHz, four times the carrier frequency generated by the difference in the optical frequencies of the laser beams. The data were then transferred to a VAX/VMS 11-750 minicomputer for FFT analysis. The data file was zero padded to a length of 32 768 data points to increase the resolution in the frequency domain. Given this sampling rate and record length, the frequency resolution was 6.1 Hz. No window was used in the computation of the FFT of the signals because the signals being analyzed are very narrow band in nature. Also, any window applied to the signal would introduce artificial broadening of the peaks in the frequency domain which may mask the broadening induced by Brownian motion.

III. RESULTS

The results from two different experiments with the LDV apparatus are presented in this section. First, the laser

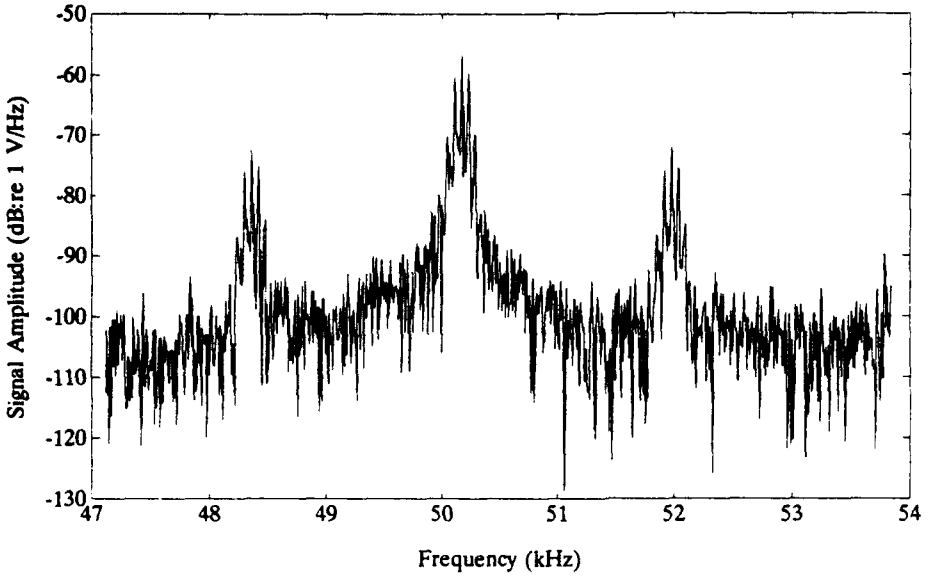

FIG. 5. Magnitude of the Fourier transform of the photomultiplier signal in the LDV detection of a harmonic wave (1809 Hz, 179 dB *re*: 1 μPa, 75.4×10^{-9}-m acoustic particle displacement) in a water-filled standing wave tube.

detection of sound in the wave tube is established and signal-to-noise ratio considerations are discussed. Second, a detailed study of signal broadening due to Brownian motion is presented.

A. Laser detection of sound

The LDV system for noninvasive detection of sound was tested with a steady time-harmonic sound wave of frequency $f_a = 1809$ Hz exciting a quarter-wavelength resonance in the water-filled standing wave tube, the upper surface being the pressure release surface. Measurements were made near the free surface of the water column where the acoustic particle velocity would be the greatest. As indicated above, the Doppler-shifted signal was captured, digitized, and stored on a minicomputer where the spectral analysis was performed. A large number of signals were recorded for different values of laser intensity and scattering microparticle size. Figure 5 shows a typical spectrum (magnitude of the Fourier transform) centered around the beat frequency of $f_d = 50$ kHz corresponding to the difference between the two Bragg frequencies. The magnitude of the Bragg peak indicates that there is indeed a clear fringe pattern in the probing volume where the two laser beams intersect. The presence of two side peaks on each side of the Bragg peak, at frequencies $f_- = f_d - f_a$ and $f_+ = f_d + f_a$, indicates that the light signal is modulated by a frequency f_a, i.e., that the scatterers are oscillating at a frequency f_a under the action of the acoustic wave. These side peaks are referred to as the acoustic peaks. Figure 5 reveals that the acoustic peak on the left is 1807 Hz below the Bragg peak frequency and that the acoustic peak on the right is 1813 Hz above the Bragg peak frequency. Hence, the LDV detection indicates that the sound wave in the water tube is at a frequency of about 1810 Hz, which agrees quite well with the measured input frequency of 1809 Hz. Apart from the frequency of the sound wave, one needs to determine its amplitude. Following the method outlined in Sec. II B, it is found from Fig. 5 that the two acoustic peaks are 15.7 and 15.5 dB lower than the central Bragg peak. Using these values in Eq. (11), we determine the amplitude of the acoustic particle displacement to be 75.4 nm or 179 dB *re*: 1 μPa. The independent measurement of the acoustic particle displacement outlined in Sec II E [see Eq. (25)] yields a value for the acoustic particle displacement of 61 nm. This measurement is made to give a rough estimate of the acoustic particle displacement and a confirmation of the LDV method. The discrepancy between the two displacement values can be explained by the difficulty of accurately measuring the volume of air trapped in the tape cylinder between the water surface and the microphone and the flexibility of the tape cylinder wall. Hence, it is clearly established from Fig. 5 that the LDV detection system allows to measure nonintrusively both the amplitude and the frequency of a time-harmonic continuous sound wave.

Figure 6 is an expanded view of the same data that are shown in Fig. 5 which reveals secondary peaks within the primary peaks (the Bragg and acoustic peaks). These peaks appear at integer multiples of 60 Hz and had the affect of modulating the photomultiplier output signal. This effect was found to be caused by the *mechanical* vibration of electrical machinery in the building that contains the prototype LDV system. Added mass on the optical rail supporting the wave tube and vibration isolation between the rail and the foundation reduced the 60-Hz components by approximately 10 dB compared to their level shown in Fig. 6. This reduction in the 60-Hz noise level was adequate for accurate determination of the half-amplitude widths of the signal peaks.

B. Signal detection threshold

The minimum detectable signal can be roughly estimated from Fig. 5 by noting that the noise level is about 40 dB

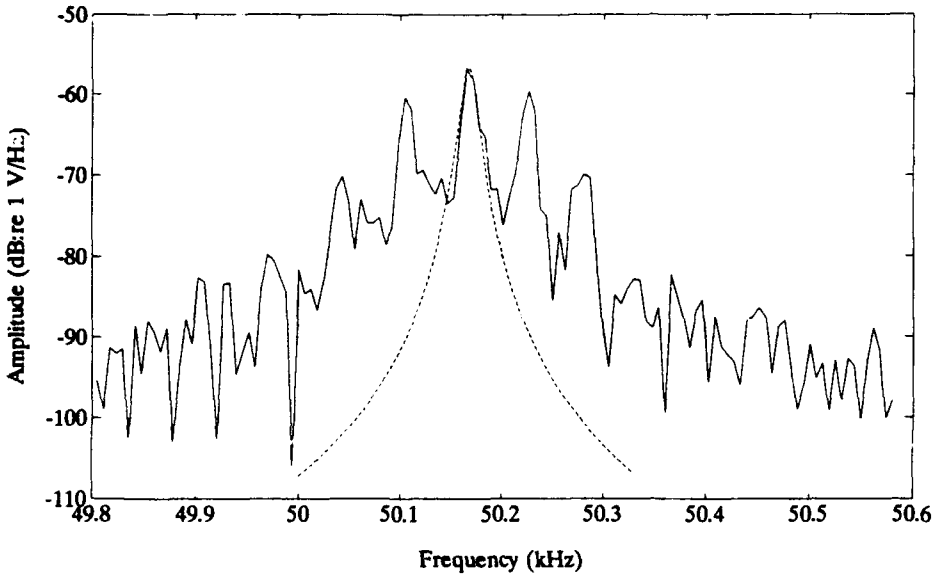

FIG. 6. The enlarged view of the Fourier transform LDV signal shows the presence of 60-cycle sidelobes. The dotted line indicates the Lorentzian curve fit used to measure the bandwidth.

below the Bragg peak. Such a value indicates that a peak acoustic particle displacement of 5 nm can be detected in water at a frequency of 1809 Hz. [See Eq. (11).] This value corresponds to a minimum detectable signal level of 154 dB *re*: 1 μPa. The question arises as to whether this minimum detectable threshold is limited by the shot noise in the photomultiplier tube. In any LDV system, the minimum detectable signal is limited in a fundamental way by the shot noise of the photomultiplier detecting the Doppler-shifted light. Hanish[6] has given an expression for the shot-noise limit in the following form:

$$A_{\min} = (\lambda h c_e B / 2\pi^2 n \eta P_0)^{1/2}, \tag{26}$$

where λ is the optical wavelength of the laser, $h = 6.6\times 10^{-34}$ J·s is Planck's constant, $c_e = 3\times 10^8$ m/s is the *in-vacuo* speed of light, B is the bandwidth of the receiving electronics, n is the index of refraction of the water, η is the quantum efficiency of the photomultiplier, and P_0 is the scattered light power incident on the sensitive surface of the photomultiplier. In our experiment, λ takes the value of 514.5 nm, the quantum efficiency is 0.22, and the bandwidth is about 10 kHz. The shot-noise limit is thus estimated to be $A_{\min} = 1.33\times 10^{-14}(P_0)^{-1/2}$. In order to estimate how far from the shot noise limit the LDV probe is actually operating, it is necessary to estimate the laser power P_0 incident on the photomultiplier. This is achieved first by relating the output voltage at the back end of the photomultiplier (measured to be about 67 mV peak to peak) to the current at the first stage of the photomultiplier. For a 800 volts bias voltage on the photomultiplier, the gain in current between the front end and the back end of the photomultiplier is 2×10^5. Since the voltage at the back end of the photomultiplier is measured across a 50 Ω resistor, the current at the front end of the photomultiplier is $i_{pm} = 1.63\times 10^{-11}$ amp. The number of electrons knocked off the photo-sensitive surface of the front end of the photomultiplier is thus $i_{pm}/q_e \simeq 10^8$ electrons per second, where $q_e = 1.6\times 10^{-19}$ coulomb is the electric charge of an electron. Since the quantum efficiency $\eta = 0.22$ is defined as the ratio of electrons produced at the first stage (front end) of the photomultiplier to the number of photons incident on the photosensitive surface, one can estimate the number of incident photons to be about 4.5×10^8 every second. But the energy E of a single photon is related to its wavelength by the relation $E = h\nu = hc/\lambda = 3.86\times 10^{-19}$ J. Therefore, the total energy per unit time incident on the photomultiplier, i.e., P_0, is $4.5\times 10^8 \times 3.9\times 10^{-19} \simeq 1.7\times 10^{-10}$ W. Inserting this value of P_0 in Eq. (26) yields an estimate of the shot-noise limited minimum peak amplitude detectable with our LDV system: $A_{\min} \simeq 1$ nm, which corresponds to a free-field sound-pressure level of 142 dB *re*: 1 μPa. This estimate can be compared with our estimate of approximately 5 nm (156 dB *re*: 1 μPa) for the minimum detectable signal at a frequency of 1809 Hz based on the signal-to-noise limitation in Fig. 5. From this comparison it may be concluded that our LDV system is operating almost at its shot-noise limit.

From Eqs. (11) and (26) it follows that the LDV technique detects particle displacement. Therefore, this technique is particularly well suited to low-frequency applications where the particle displacements are large for a given acoustic pressure. This is because, for a monochromatic plane wave propagating in free space, the ratio of acoustic particle displacement to the acoustic pressure is inversely proportional to the frequency and hence the minimum detectable sound pressure is inversely proportional to the acoustic pressure. The minimum detectable signal level also depends on the scattered light power P_0. Therefore, the minimum detectable level is a function both of the microparticle size and optical properties, and of the scattering direction along which light is collected by the receiving optics. The minimum level estimates given in subsection B for a polystyrene microparticle have been both measured and calculated.[2]

These results for the minimum detectable signal were

established for the system in the forward scatter configuration which is appropriate when collecting data in an impedance tube. In other applications it may be more appropriate to use a backscatter arrangement.

Typically, the backscatter cross section is significantly smaller than the cross section for forward scatter. For example, from the data given by Drain, it is that for microparticles of diameter $\geqslant 1\ \mu$m the backscatter light intensity is lower by approximately two orders of magnitude compared to the light scattered in the forward direction. However, the low value of the backscatter cross section can be compensated by using a higher intensity incident light beam.

C. Broadening due to Brownian motion

A systematic study of the spectral broadening caused by Brownian motion of the microparticles in suspension was undertaken in order to answer the following question: Is Brownian motion a limiting factor in the LDV detection of underwater sound? The question arises because Hanish, in his preliminary study of the laser hydrophone,[6] estimated the spectral broadening due to Brownian motion to be

$$B_H = 16\pi n^2 k_B T/3\lambda^2 \mu a, \tag{27}$$

where $k_B = 1.38\times 10^{-23}$ N m K^{-1} is Boltzmann's constant, T is the absolute temperature of the water, λ is the optical wavelength, n is the index of refraction of water (viscosity $\mu = 10^{-3}$ N m^{-2} s), and a is the radius of the microsphere in suspension. Hanish's prediction is shown in Fig. 7 as a solid line as a function of particle radius. It shows that, for microparticles of 0.1-μm radius, the broadening is anticipated to be as high as 4.5 kHz. In other words, the width of the Bragg peak would completely obliterate any acoustic signal at frequencies below 4.5 kHz in the LDV detection scheme. It turns out that, as is shown below, our experimental data do not support Hanish's prediction.

Data were recorded following the procedure described in Sec. II F with calibrated microparticles of radii 0.1, 1, and 10 μm in suspension in reverse osmosis purified water. In each case, a curve fit based on a three parameter nonlinear least-squares was computed to match the measured Bragg peak. An example is shown in Fig. 6. Figure 7 shows the experimentally measured half-amplitude (6 dB) width of the peaks found by averaging about ten different measurements of the bandwidth for each particle size. These widths were found to be 20, 19, and 18 Hz, respectively. These values are below the predicted minimum broadening B_H given by Eq. (27) which cannot, therefore, be taken as a good model for spectral broadening. In fact, Eq. (24), which is based on Clark's model (shown in Fig. 7 as a dashed line), seems more appropriate because it does not contradict our experimental data. Since it is found experimentally that spectral broadening is about 20 Hz for particle radii ranging from 0.1–10 μ, (i.e., it seems independent of particle radii for radii greater than 0.1 μm), one can ascertain that Brownian motion is not the cause of the observed spectral width. Instead, it is probable that other causes such as the slow drift of the microparticles in suspension, or the finite length of time over which the data are Fourier transformed, or fluctuations in the frequency synthesizers driving the Bragg cells, are really the limiting factors in the measured spectral broadening. Since the mean particle diameter in the ocean is several microns, the experiment discussed above (which covers two decades in particle size around 1 μm) indicates that Brownian motion is unlikely to be a limiting factor in the laser detection of underwater sound.

IV. CONCLUSIONS

A differential heterodyne laser Doppler velocimeter has been assembled and tested to measure nonintrusively small perturbation associated with acoustic standing waves excit-

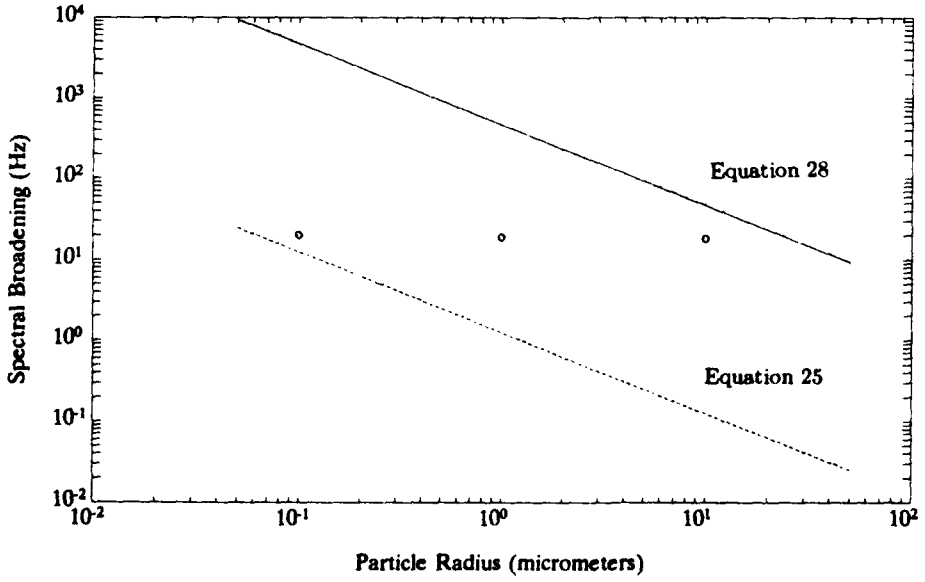

FIG. 7. Spectral broadening due to Brownian motion as a function of scatterer radius. Solid line: Hanish's prediction [Eq. (27)]; dashed line: Clark's prediction [Eq. (24)]; and experimental results (circles).

ed by a piezoelectric transducer in a standing wave tube filled with water. An important factor in the design of the LDV system was to decouple with optical fibers the optical bench from the standing wave tube so as to ensure maximum flexibility for future applications. Significant improvement in signal-to-noise ratio was obtained by using polarization preserving single mode fibers in the two arms of the interferometer. Also, fairly efficient coupling of light in and out of the fibers was achieved by using miniature lenses with graded index of refraction (GRIN lenses). It was found that spectral analysis of the signal detected at the receiver directly performed on a spectrum analyzer is not a very efficient way to analyze the data. Instead, it is recommended to capture the signal whenever a strong burst of scattered light occurs (i.e., whenever a microparticle drifts into the fringe volume where the two laser beams intersect) and to digitize the signal and store it in a microcomputer for fast Fourier transform analysis. It was found that our LDV prototype is able to detect acoustic particle displacement as small as 5 nm with a detection bandwidth of 10 kHz. This detection threshold corresponds to 156 dB *re*: 1 μPa at 1.8 kHz, and decreases even further at lower frequencies, and with narrower bandwidth of the receiving electronics. The shot-noise limit of the prototype was estimated to be such that the minimum detectable particle displacement is of the order of 1 nm. Our LDV probe is thus operating very close to its shot-noise limit. A systematic study of the spectral broadening due to Brownian motion was carried out with calibrated microspheres of radii 0.1, 1, and 10 μm in suspension in reverse osmosis filtered water. It was found that Brownian motion is not a serious limitation for detection of sound in water containing scatterers whose radii is greater than 0.1 μm. Furthermore, laser detection of sound in air is much easier because particle displacements in air are much larger than particle displacements in water. Further improvements of the LDV prototype include the configuration of the system into a backscattering mode for operations in a water tank where the detection of acoustic transients is made possible by using a phase-locked loop.

ACKNOWLEDGMENTS

The authors would like to express their gratitude to Allan D. Pierce for enlightening comments during the course of this research. This work was supported by the Office of Naval Research as part of Joseph Vignola's doctoral dissertation.

[1] H. Yeh and H. Z. Cummins, "Localized Fluid Flow Measurements with a He–Ne Laser Spectrometer," Appl. Phys. Lett. **4**, 176–178 (1964).
[2] L. E. Drain, *The Laser Doppler Technique* (Wiley, Chichester, 1980).
[3] W. K. George and J. L. Lumley, "The Laser-Doppler Velocimetery and Its Application to the Measurement of Turbulence," J. Fluid Mech. **60**, 321–362 (1973).
[4] K. J. Taylor, "Absolute Measurement of Acoustic Particle Velocity," J. Acoust. Soc. Am. **59**, 691–694 (1976).
[5] K. J. Taylor, "Absolute Calibration of Microphones by a Laser-Doppler Technique," J. Acoust. Soc. Am. **70**, 939–945 (1981).
[6] S. Hanish, "Underwater Laser Doppler Hydrophone," *A Treatise on Acoustic Radiation, Vol. II* (Naval Research Laboratory, Washington, DC, 1983), Chap. 6, pp. 377–397.
[7] P. S. Dubbelday and H. C. Schau, J. Acoust. Soc. Am. **86**, 891–894 (1989).
[8] J. Jarzynski, D. Lee, J. Vignola, Y. H. Berthelot, and A. D. Pierce, "Fiber-optic Doppler Systems for Remote Sensing of Fluid Flow," Proc. SPIE **925**, 250–254 (1988).
[9] J. Vignola, Y. H. Berthelot, and J. Jarzynski, "Nonintrusive absolute measurements of acoustic particle velocity in fluids," *Proceedings of the 13th International Congress on Acoustics*, edited by P. Pravica (Dragan Srnic, Sabac, Yugoslavia, 1989), Vol. 4, pp. 45–48.
[10] O. Brandt, H. Freund, and E. Hiedemann, "Schwebstoffe im Schallfeld," Zeits. Phys. **104**, 511–533 (1937).
[11] C. M. Penney, "Differential Doppler Velocity Measurements," Appl. Phys. Lett. **16**, 167–169 (1970).
[12] L. Lading, "Differential Doppler Heterodyning Technique," Appl. Opt. **10** 1943–1949 (1970).
[13] M. Abramowitz and I. Stegun, *Handbook of Mathematical Functions* (Dover, New York, 1965), p. 361.
[14] N. A. Clark and J. H. Lunacek, "A Study of Brownian Motion Using Light Scattering," Am. J. Phys. **37**, 853–855 (1969).
[15] N. A. Clark, J. H. Lunacek, and G. B. Benedek, "A Study of Brownian Motion Using Light Scattering," Am. J. Phys. **38**, 575–585 (1970).
[16] P. Morse, *Thermal Physics* (Benjamin/Cummings, Reading, MA, 1969), 2nd ed., p. 233.
[17] A. Einstein, *Investigations on the Theory of the Brownian Movement* (Dover, New York, 1956), p. 16.
[18] A. Papoulis, *Probability, Random Variables, and Stochastic Processes* (Mc-Graw Hill, New York, 1984), p. 344.
[19] L. D. Landau and E. M. Lifshitz, *Fluid Mechanics* (Pergamon, London, 1959), p. 66.
[20] A. Einstein, *Investigations on the Theory of the Brownian Movement* (Dover, New York, 1956), p. 12.
[21] F. Reif, *Fundamentals of Statistical and Thermal Physics* (McGraw-Hill, New York, 1965), p. 585.
[22] C. Kittel, *Elementary Statistical Physics* (Wiley, London, 1958), p. 131.
[23] A. Yariv, *Optical Electronics* (Holt, Rinehart and Winston, New York, 1985), Chap. 12.
[24] I. Kaminow, "Polarization in Optical Fiber," IEEE J. Quant. Electron **QE-17** (1), 15–21 (1981).
[25] A. Snyder, "Understanding Monomode Optical Fibers," Proc., IEEE **69** (1), 6–13 (1981).
[26] W. Eickhoff, "Temperature Sensing by Mode-Mode Interference in Birefringent Optical Fibers," Opt. Lett. **6**, 204–206 (1981).
[27] E. Marchand, *Gradient Index Optics* (Academic, New York, 1978).
[28] W. Kuhl, E. Meyer, H. Oberst, E. Skudrzyk, and K. Tamm, *Sound Absorption and Sound Absorbers*, translated from German in 1947 by Charles Mongan for the Department of the Navy, Bureau of Ships, pp. 382–391.
[29] A. D. Pierce, *Acoustics: An Introduction to Its Physical Principles and Applications* (McGraw-Hill, New York, 1981), p. 317.
[30] Particles manufactured by Duke Scientific Corporation, 1135D San Antonio Road, Palo Alto, CA 94303.